Magnetic ordering and hybridisation in YbAuCu 4

P. Bonville, B. Canaud, J. Hammann, J. Hodges, P. Imbert, G. Jéhanno, A. Severing, Z. Fisk

Classification
Physics Abstracts
71.28 — 75.30M — 76.80

Magnetic ordering and hybridisation in $YbAuCu_4$

P. Bonville([1]), B. Canaud([1]), J. Hammann([1]), J.A. Hodges([1]), P. Imbert([1]), G. Jéhanno([1]), A. Severing([2]) and Z. Fisk([3])

([1]) Service de Physique de l'Etat Condensé, Département de Recherche sur l'Etat Condensé, les Atomes et les Molécules, Centre d'Etudes de Saclay, 91191 Gif-sur-Yvette, France

([2]) Institut Laue-Langevin, 38042 Grenoble, France

([3]) Los Alamos National Laboratory, Los Alamos, New Mexico 87545, U.S.A.

(Received 25 October 1991, accepted in final form 18 December 1991)

Résumé . — Nous présentons une étude par spectroscopie Mössbauer sur ^{170}Yb des propriétés à basse température du composé cubique à électrons lourds $YbAuCu_4$. Dans la phase antiferromagnétique ($T_N = 1$ K), nous mesurons une réduction de 20 % du moment spontané à saturation de Yb^{3+} par rapport au moment de l'état fondamental Γ_7 de champ cristallin, et nous mettons en évidence une anisotropie notable de l'interaction magnétique entre les ions. Nous interprétons ce comportement en termes d'hybridation entre les électrons 4f et les électrons de conduction, qui rend compte des propriétés de type électron lourd. L'échelle d'énergie $k_B T_0$ de l'hybridation est estimée de l'ordre de 0,3 K. Les spectres Mössbauer dans les phases ordonnée et paramagnétique présentent des élargissements de raie inhomogènes qui sont interprétés en termes de distribution de contraintes locales suivant les axes <111> du cristal, d'énergie magnéto-élastique moyenne 0,2 – 0,4 K.

Abstract . — We report on a ^{170}Yb Mössbauer spectroscopy investigation of the low temperature magnetic properties of the cubic heavy electron material $YbAuCu_4$. In the antiferromagnetically ordered phase ($T_N = 1$ K), we measure a 20 % reduction of the Yb^{3+} saturated spontaneous moment with respect to that of the crystal field Γ_7 ground state and we evidence a sizeable anisotropy of the interionic magnetic interaction. We interpret these features in terms of 4f electron - conduction electron hybridisation, which accounts for the heavy electron properties. The energy scale $k_B T_0$ of hybridisation is estimated to be 0.3 K. The Mössbauer spectra in the ordered and paramagnetic phases show inhomogeneous line broadenings which are interpreted as arising from a distribution of local strains along the ⟨111⟩ crystal axes, of mean magneto-elastic energy 0.2 – 0.4 K.

1. Introduction.

The intermetallic compounds with Ce, Yb or U can present non-standard transport and magnetic properties at low temperature which are thought to be related to the presence of hybridisation between the localised f electrons and the itinerant band electrons [1,2]. The energy scale for hybridisation is called the Kondo temperature T_0; for $T < T_0$, the properties of the material strongly deviate from those of an array of localised trivalent Ce or Yb ions (with total angular momentum **J**), weakly coupled to band electrons (with spin **s**) through the conventional k – f exchange interaction:

$$\mathcal{H}_{kf} = -2J_{kf}\mathbf{s}.\mathbf{J}, \tag{1}$$

where J_{kf} is the "atomic" exchange integral.

For temperatures below T_0, hybridisation leads to the formation of a narrow band located near the Fermi level and of width of order $k_B T_0$, where the quasi-particles have predominantly 4f character and are strongly correlated. Depending on the structure and symmetry properties of the energy bands, the charge carriers at the Fermi level may show high effective masses, varying roughly as $1/T_0$; in the so-called "heavy electron" compounds where the Kondo temperature is low, the mass enhancement can reach values of a few 100.

In the limit of weak hybridisation, charge fluctuations are negligible and the compound is called a Kondo lattice, the rare earth ions being trivalent to a good approximation. The ground state of a Kondo lattice depends on the relative magnitudes of T_0 and of the energy scale of the interionic magnetic coupling, as was first shown by Doniach [3]. The interionic coupling induced by hybridisation has a RKKY-like dependence upon distance [4] and can be considered as an effective interionic exchange T_{RKKY}; it favours a ground state with long range ordering of the 4f magnetic moments, whereas hybridisation, which induces local quantum fluctuations of the 4f moment with time scale $\hbar/k_B T_0$, has an on-site demagnetising effect. So, when $T_0 \gg T_{RKKY}$, a non-magnetic ground state results, which behaves like a Fermi liquid for $T < T_0$. A magnetically ordered ground state occurs when the quantum fluctuations do not entirely smear out intersite magnetic correlations, i.e. when $T_0 \lesssim T_{RKKY}$. In this case, the magnetically ordered phase can show unconventional features: the actual ordering temperature T_N can be drastically reduced with respect to T_{RKKY}; the 4f saturated magnetic moment can be smaller than that expected for the crystal electric field (C.E.F.) ground state of the ion; the anisotropy of the interionic interaction can be strong even in compounds with cubic symmetry; the magnetic ordering can show unusual structures. In the present state of knowledge, however, the occurence of one or more of these properties in a given material cannot be predicted with certainty.

The determination of the saturated magnetic moment, of the magnetic energy $k_B T_{RKKY}$ and of the magnetic anisotropy in hybridised compounds is thus of great interest for a better understanding of the magnetic ground state formation. In Yb based compounds, a local measurement technique such as ^{170}Yb Mössbauer spectroscopy can provide such information, as demonstrated by the Mössbauer investigation of the cubic monopnictides YbP and YbAs [5, 6], which are hybridised materials with a magnetic ground state ($T_N \simeq 0.7$ K). In these compounds, hybridisation leads to a reduction of the Yb saturated moment and of the transition temperature T_N, but the magnetic anisotropy is found to be much smaller than the exchange interaction.

In another series of cubic Yb based intermetallics, $YbXCu_4$, where X = Ag, Au and Pd, specific heat, resistivity and magnetic measurements have evidenced "heavy electron" behaviour [7]. Among these compounds, $YbAgCu_4$ appears to have the highest Kondo temperature ($T_0 = 110$ K) [8] and it has a non-magnetic ground state. In contrast, $YbAuCu_4$ and $YbPdCu_4$

show a specific heat peak below 1 K, attributed to the occurence of a magnetic phase transition. Hence we expect that hybridisation is much less important in these two compounds than in $YbAgCu_4$ and that the C.E.F. energy levels of the Yb^{3+} ion are well defined in $YbAuCu_4$ and $YbPdCu_4$. Crystal field transitions have indeed been observed and analysed in these materials by an inelastic neutron scattering study [9, 10]. The cubic C.E.F. interaction partially lifts the degeneracy of the $J = 7/2$ ground spin-orbit multiplet of the Kramers Yb^{3+} ion into two doublets Γ_6 and Γ_7, and a quartet Γ_8. The C.E.F. level scheme proposed in reference [9] for Yb^{3+} in $YbAuCu_4$ consists of a Γ_7 ground state, the excited states being Γ_8 and Γ_6 respectively at energies 45 K and 80 K above the ground state.

We present in this work ^{170}Yb Mössbauer spectroscopy measurements together with magnetic susceptibility and magnetisation data at low temperature in $YbAuCu_4$; we confirm the presence of an antiferromagnetic transition at $T_N \simeq 1$ K, and we analyse the properties of the magnetically ordered phase in terms of hybridisation of the ground state. We could estimate the Kondo temperature of $YbAuCu_4$, the interionic exchange energy and we evidenced the presence of a sizeable magnetic anisotropy. We analyse hybridisation in terms of a model derived from the Noncrossing Approximation (N.C.A.) solution of the Anderson Hamiltonian [11].

Another feature of Mössbauer spectroscopy is that it is very sensitive to small deformations of the ionic environment; the Mössbauer spectra in $YbAuCu_4$ show noticeable line broadenings which we attribute to a distribution of small distortions of the Yb site in our sample.

This paper is organized as follows: section 2 deals with the sample characterisation by means of x-ray diffraction spectra. Section 3 describes the experimental setup, and section 4 reports on the zero applied field Mössbauer spectra in the magnetically ordered phase. In section 5, the $T = 0.05$ K Mössbauer spectrum is thoroughly analysed in terms of crystal field distortions and weak hybridisation of the Yb ion 4f electrons with band electrons. Section 6 contains the Mössbauer data obtained in applied magnetic fields in the antiferromagnetic phase and their interpretation. In section 7 we describe the results obtained in the paramagnetic phase: Mössbauer spectra in zero applied field as well as in high magnetic fields, and magnetisation and susceptibility measurements. Finally, section 8 contains a discussion of the results.

2. Sample characterisation.

The $YbAuCu_4$ sample used for the present experiments is part of the sample prepared for the neutron inelastic scattering experiments [9]. Following the x-ray and neutron diffraction patterns [10], all three compounds $YbAgCu_4$, $YbAuCu_4$ and $YbPdCu_4$ crystallize in the cubic C15b structure (space group $F\bar{4}3m$). The x-ray powder pattern of $YbAuCu_4$ using filtered Cu radiation shows a weak impurity line at an angle $2\theta \simeq 50°$, which does not pertain to the diffraction pattern of the oxyde Yb_2O_3. The impurity content of the $YbAuCu_4$ sample is thus of the order of a few percent.

The C15b structure is closely related to the C15 $MgCu_2$-type structure (space group Fd3m); the Yb and metal (Ag, Au or Pd) atoms, occupying respectively the positions (0,0,0) and (1/4,1/4,1/4) in the cubic cell, form two fcc lattices translated from each other by the vector (1/4,1/4,1/4) **a**, where **a** is the fcc cell basis vector. The Cu atoms occupy the positions (xxx), $(x\bar{x}\bar{x})$, $(\bar{x}x\bar{x})$ and $(\bar{x}\bar{x}x)$, where x is a free parameter. According to x-ray intensity calculations, the value of x in the three compounds should not be very different from its value 5/8 in the C15 structure. The (200) diffraction line, which is not allowed in the C15 structure, but possible in the C15b structure, appears generally in the x-ray diffraction patterns of $YbAgCu_4$ and $YbPdCu_4$, but is absent in that of $YbAuCu_4$ [9]. This extinction is accidental and due to the

fact that the x-ray diffusion factors of Yb^{3+} and Au are not very different: $f(Yb^{3+}) = 63$ and $f(Au) = 70$ at small reflection angles.

In the C15b structure of $YbAuCu_4$, the Yb site has cubic symmetry; with $x = 5/8$, its nearest neighbours are 12 Cu atoms at a distance $a\sqrt{11}/8 \simeq 0.41a$. The next-nearest neighbours are 4 Au atoms located on the vertices of a tetraedron along the <111> directions, at a distance $a\sqrt{3}/4 \simeq 0.43a$ from the Yb site. The Yb ion is thus surrounded by 16 almost equidistant metal atoms; this high coordination environment has the <111> directions as symmetry axes.

The cubic lattice parameter reported in reference [9] for $YbAuCu_4$ is $a = 7.0519$ Å. We performed a more detailed structural analysis of our sample. An x-ray diffractometer spectrum of 100 mg of finely powdered material shows that the lines at high reflection angles are relatively broad, which is indicative of a distribution of lattice parameters. An estimation of the width of this distribution leads to: 7.033 Å $\leq a \leq$ 7.055 Å. However a Debye-Scherrer pattern performed on a small fragment of the sample shows that the material is very well crystallised with a unique lattice parameter, this parameter depending on the chosen fragment. We tentatively attribute this parameter distribution to slight stoichiometry variations within the sample, which could be due to the large number of meltings necessary to prepare the quantity of material (50 g) required for the neutron measurements [9, 10].

Therefore, there exists a small parameter inhomogeneity from grain to grain in our $YbAuCu_4$ sample, each grain being well crystallized with a well-defined cubic lattice parameter.

3. Experimental setup.

The magnetic measurements were performed using a standard extraction technique. The magnetisation curve was obtained at $T = 4.2$ K for fields up to 4.6 T. The magnetic susceptibility measurements were performed between 0.5 K and 30 K at low fields: $H = 13.6$ Oe for $T < 3$ K and $H = 136$ Oe at higher temperatures.

The ^{170}Yb Mössbauer transition has an energy of 84.3 keV and links the ground nuclear state with spin $I_g = 0$ and the excited state with spin $I = 2$. The Mössbauer spectra were recorded using a neutron-irradiated Tm^*B_{12} γ-ray source mounted on a triangular velocity drive. The linewidth of the Tm^*B_{12} source *versus* a reference $YbAl_3$ absorber is 2.7 mm/s (for ^{170}Yb, 1 mm/s = 68 MHz).

The Mössbauer experiments in zero applied magnetic field were performed in the temperature range 0.05−60 K. Experiments with an applied magnetic field up to 7 T were performed at $T = 0.05$ K and $T = 4.2$ K. The field direction was parallel to the γ-ray propagation direction. Spectra below 1 K were obtained using a ^3He−^4He dilution refrigerator.

4. Mössbauer spectra in the magnetically ordered phase in zero applied field.

4.1 SPECTRUM AT $T = 0.05$ K. — The ^{170}Yb absorption spectrum at $T = 0.05$ K (Fig.1) shows five resolved lines indicating the presence of a hyperfine field at the nucleus, and thus of magnetic ordering of the Yb^{3+} magnetic moments at this temperature. Such a spectrum, where the energy differences between adjacent lines are almost the same, can be fitted to a hyperfine Hamiltonian consisting of a dominant magnetic term and a small electric quadrupolar term:

$$\mathcal{H}_{hf} = -g_n \mu_n I_Z H_{hf} + \alpha_Q^Z \left[I_Z^2 - \frac{I(I+1)}{3} \right] \qquad (2)$$

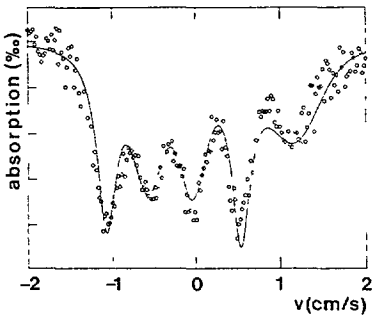

Fig. 1. — ^{170}Yb Mössbauer absorption spectrum in $YbAuCu_4$ at $T = 0.05$ K; the solid line is a fit with hyperfine Hamiltonian (2) using linearly correlated Gaussian distributions of H_{hf} and α_Q^Z with $A = 3.1 \times 10^{-2}$ mm/s/T and $B = -4.4$ mm/s (see text).

In this expression, the Z-quantisation axis is taken to be along the hyperfine field $\mathbf{H}_{hf}$ and $g_n\mu_n\mathbf{I}$ is the magnetic moment of the excited nulear state ($I = 2$). The quadrupolar parameter α_Q^Z is defined as: $\alpha_Q^Z = \frac{eQV_{ZZ}}{8}$, where Q is the nuclear electric quadrupole moment and $V_{ZZ} = V_{zz}.\frac{3\cos^2\theta - 1}{2}$ is the projection onto the hyperfine field direction OZ of the principal component V_{zz} of the electric field gradient (E.F.G.) tensor at the Yb site, θ being the angle between OZ and the principal axis z of the E.F.G. tensor. Such an expression for the hyperfine quadrupolar interaction holds only when it can be considered as a perturbation on the magnetic hyperfine interaction. The small value found for the quadrupolar parameter in $YbAuCu_4$ shows that the Yb ion lies at a site with cubic or quasi-cubic symmetry.

The fitted parameters at 0.05 K are: $H_{hf} = (148.5 \pm 3)$T and $\alpha_Q^Z = (0.25 \pm 0.1)$mm/s. The hyperfine field in a metallic host comes mostly from the 4f Yb electrons, and is proportional to the 4f magnetic moment μ : $H_{hf}^{4f} = C\ \mu$, where $C = (102 \pm 3)\text{T}/\mu_B$ for $^{170}Yb^{3+}$[12]. There is an extra contribution coming from the conduction electron polarisation which is an order of magnitude smaller than H_{hf}^{4f}, and which will be shown to be negligible in $YbAuCu_4$ (see Sect. 7.3). Therefore, the saturated spontaneous magnetic moment of the Yb^{3+} ion is: $\mu(0.05\text{ K}) = (1.46 \pm 0.07)\mu_B$.

The cubic C.E.F. eigenstates Γ_6 and Γ_7 have magnetic moments $\mu(\Gamma_6) = 1.33\mu_B$ and $\mu(\Gamma_7) = 1.715\mu_B$, and zero associated E.F.G. tensor. In the presence of an exchange (or Zeeman) interaction, mixing of the Γ_8 state into the ground doublet enhances the saturated moment and creates a small positive induced E.F.G. at the Yb site. At first approximation, the experimental values of μ and α_Q^Z are consistent either with a Γ_6 ground state or with a Γ_7 ground state with a reduced magnetic moment. The latter possibility is in agreement with the inelastic neutron scattering determination [9, 10] and the reduction of the saturated moment could then be due to 4f electron-band electron hybridisation. The possibility of a Γ_8 quartet as the ground state will be examined and ruled out in section 8 and the nature of the Yb^{3+} ground state will be further discussed in section 6.

Another feature of the $T = 0.05$ K spectrum is the presence of inhomogeneous broadening of the lines as can be seen in figure 1. This is the hallmark of a distribution of hyperfine parameters. In the case of only a distribution of the hyperfine fields, the broadenings would be symmetrical with respect to the central line; the observed asymmetry of the linewidths is caused by a correlated distribution of hyperfine fields and electric field gradients. This property

is easily understood using the expressions of the hyperfine energies of Hamiltonian (2):

$$E(m) = -g_n\mu_n H_{hf} m + \alpha_Q^Z(m^2 - 2), \tag{3}$$

where m is the z-component of the nuclear spin ($-2 \leq m \leq 2$). Then, for a small variation of H_{hf} and α_Q^Z :

$$\Delta E(m) = -g_n\mu_n m\Delta H_{hf} + (m^2 - 2)\Delta\alpha_Q^Z, \tag{4}$$

with $g_n\mu_n > 0$. Inspection of this formula shows that, if ΔH_{hf} and $\Delta\alpha_Q^Z$ are correlated, for instance positively, then for the less energetic line ($m = 2$), the two contributions to $\Delta E(m)$ are of opposite sign, whilst for the most energetic line ($m = -2$) they have the same sign. This leads to broadenings of the type experimentally observed, for instance the linewidth $G(m = 2) = 3.2$ mm/s is much smaller than $G(m = -2) = 6.2$ mm/s. We have fitted the $T = 0.05$ K spectrum using correlated distributions of H_{hf} and α_Q^Z with Gaussian shape. The correlation is taken to be linear:

$$\alpha_Q^Z = A\ H_{hf} + B, \tag{5}$$

which, as will be shown in section 5, is the form to first order perturbation in presence of distortions from cubic symmetry of the Yb site. The solid curve in figure 1, which represents such a fit where the intrinsic Mössbauer linewidth is fixed at the minimal experimental value 2.7 mm/s, shows that the inhomogeneous broadenings are correctly reproduced. The fitted gaussian distribution of hyperfine fields has the following characteristics: mean value $H_{hf}^0 =$ 148.5T and mean square deviation $\Delta H_{hf} = (19 \pm 2.5)$T. The A and B parameters of the correlation can be allowed to vary substantially without much affecting the quality of the fit. One finds that the acceptable values for A (in mm/s/T) and B (in mm/s) are linearly related:

$$B = 0.21 - 1.47 \times 10^2 A, \tag{6}$$

the coefficient A varying in the range: $1.5 \times 10^{-2} \leq A \leq 3.2 \times 10^{-2}$, yielding $-4.5 \leq B \leq -2$ (see Fig. 3). The center of the distribution of quadrupolar parameters is quasi-independant of the A and B values and is worth: $\alpha_Q^0 = 0.25$ mm/s; the mean square deviation $\Delta\alpha_Q$ varies from 0.34 mm/s (for $A = 1.5 \times 10^{-2}$) to 0.52 mm/s (for $A = 3.2 \times 10^{-2}$). We performed detailed perturbation calculations of the A and B coefficients as a function of the type of C.E.F. distortions for the two cases of a Γ_6 or Γ_7 C.E.F. ground state: these calculations and comparison with experiment will be explained in section 5.

4.2 THERMAL VARIATION OF THE HYPERFINE FIELD AND THE MAGNETIC TRANSITION. — The hyperfine field smoothly decreases from 148.5 T at 0.05 K to 110 T at 0.8 K, its thermal variation matching with the mean field curve for $S = 1/2$ with $T_N = 1 \pm 0.1$ K (Fig.2). Above 0.8 K the spectra show no resolved structure and the overall linewidth decreases upto 1.2 K. The magnetic transition is very probably of second order, the transition temperature lying between 0.8 K and 1.2 K. The low temperature magnetic susceptibility shown in the insert of figure 2 confirms this conclusion: it presents a kink characteristic of a transition to an antiferromagnetic phase with $T_N = 1$ K. This result is at variance with that reported in reference [7] where the specific heat peak found in the $YbAuCu_4$ sample is located near 0.6 K.

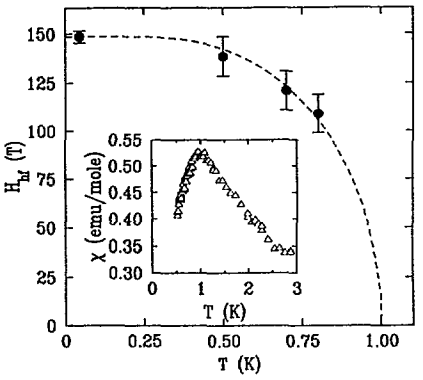

Fig. 2. — Thermal variation of the hyperfine field on ^{170}Yb in YbAuCu$_4$; the dashed line is the $S = 1/2$ mean field curve with $H^0_{hf} = 148.5$T and $T_N = 1$ K. Insert: low temperature magnetic susceptibility in YbAuCu$_4$ ($H = 13$Oe).

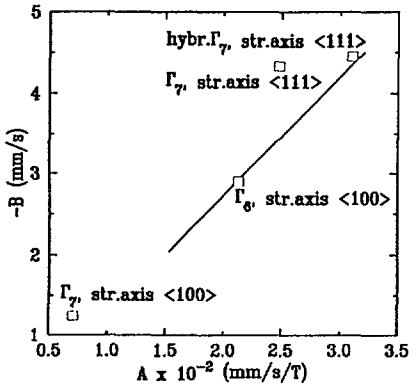

Fig. 3. — Coefficients of the linear correlation between H and α^Z_Q in YbAuCu$_4$ at $T = 0.05$ K : $\alpha^Z_Q = AH_{hf} + B$; the solid line represents the experimentally acceptable values of A and B (expression (5)); the squares represent the calculated values for a Γ_6 or a Γ_7 ground state and for a strain axis along <100> or <111> (see Tab. II).

5. Analysis of the spectrum at T=0.05 K; hybridisation and C.E.F. distortions.

In this section, we shall examine the combined effects of the exchange interaction and of small distortions from cubic symmetry (strains) on the ^{170}Yb hyperfine spectrum in the magnetically ordered phase. We shall show that the inhomogeneous broadenings of the $T = 0.05$ K spectrum can be interpreted by assuming the presence of a distribution of strains at the Yb site along a well defined symmetry axis.

We treat the exchange interaction $\mathcal{H}_{ex}$ and the C.E.F. distortion interaction $\mathcal{H}_{dis}$ in perturbation with respect to the cubic C.E.F. interaction. This is justified since the lowest C.E.F. excitation has an energy of 45 K [9], $\mathcal{H}_{ex} \sim k_B T_N = 1$ K and $\mathcal{H}_{dis}$, as is shown below, is of the order of a few 0.1 K. To first order perturbation, $\mathcal{H}_{ex}$ and $\mathcal{H}_{dis}$ can be treated independantly.

As will be shown in section 7.1, the mean value of $\mathcal{H}_{dis}$ is zero: $\langle\mathcal{H}_{dis}\rangle = 0$, i.e. there is no average non-zero strain in the sample. We can then analyse the mean values of H_{hf} and α_Q^Z in the saturated state at $T = 0.05$ K in terms of the exchange interaction alone and then examine the effects of the strains described by $\mathcal{H}_{dis}$.

5.1 MIXING DUE TO THE EXCHANGE FIELD. — At $T = 0.05$ K, the ground doublet is split by the exchange interaction:

$$\mathcal{H}_{ex} = g_J \mu_B \mathbf{J}.\mathbf{H}_{ex}, \tag{7}$$

where $\mathbf{H}_{ex}$ is the exchange field which we assume is directed along the antiferromagnetic sublattice moment direction OZ. Mixing of the Γ_8 state into the ground doublet (there is no matrix element of $\mathbf{J}$ between Γ_6 and Γ_7) to first order perturbation enhances the magnitude of the magnetic moment $\mu = -g_J \mu_B \langle J_Z \rangle$ in an isotropic way:

$$\mu = \mu(\Gamma_i)(1 + P\varepsilon) \qquad i = 6, 7. \tag{8}$$

In this expression, ε is the perturbation parameter: $\varepsilon = g_J \mu_B H_{ex}/\Delta_8$, Δ_8 being the Γ_8 excitation energy, and P is a number independent of the direction of $\mathbf{H}_{ex}$ but depending on the nature (Γ_6 or Γ_7) of the unperturbed ground state. Mixing also induces an axially symmetric E.F.G. at the Yb site, with its principal component along the direction of $\mathbf{H}_{ex}$; the associated quadrupolar parameter is, to first order perturbation:

$$\alpha_Q^Z = A_Q \left\langle 3J_Z^2 - J(J+1) \right\rangle = R(\mathbf{u}) A_Q \varepsilon, \tag{9}$$

where $A_Q = 0.276$ mm/s for ^{170}Yb and $R(\mathbf{u})$ depends upon the orientation of the exchange field represented by the unit vector $\mathbf{u}$ and on the nature of the ground state.

We shall compare the experimental values $\mu = (1.46 \pm 0.07)\mu_B$ and $\alpha_Q^Z = (0.25 \pm 0.1)$mm/s with (8) and (9) in the two hypotheses of a Γ_6 or Γ_7 ground doublet. Details concerning the calculation of P and $R(\mathbf{u})$ are given in Appendix 1.

For a Γ_6 doublet, $\mu(\Gamma_6) = 1.33\mu_B$ and $P = 20/3$. The quantity $R(\mathbf{u})$ has its minimum value $O(\varepsilon^2)$ when $\mathbf{H}_{ex}$ is along <111> and its maximum value 70 when $\mathbf{H}_{ex}$ is along <100>. Using the value $\Delta_8 = 45$ K, we find that an exchange field $H_{ex} \simeq 0.87$ T accounts for the experimental μ value and yields an acceptable value for α_Q^Z when $\mathbf{H}_{ex}$ is along the <100> direction.

For a Γ_7 doublet, $\mu(\Gamma_7) = 1.715\mu_B$ and $P = 4$. The quantity $R(\mathbf{u})$ has its maximum value 48 when $\mathbf{H}_{ex}$ is along <111> and its minimum value 18 when $\mathbf{H}_{ex}$ is along <100>. The experimental μ value is 15 % smaller than the bare $\mu(\Gamma_7)$ and is even smaller than the exchange enhanced value $\mu(\Gamma_7)(1+4\varepsilon)$. Hybridisation of 4f electrons with band electrons, which is known to be present in $YbAuCu_4$ [7], can account for such a reduction. We shall use here a simplified model [11] in order to compute the moment reduction. In this model, the effect of a weak hybridisation is merely to assign an occupation number n_i to each hybridised electronic level; this occupation number is given, at $T = 0$ K, by the expression:

$$n_i = \frac{(1 - n_f)\Gamma}{\pi(T_0 + \Delta_i)}. \tag{10}$$

where T_0 is the Kondo temperature, Γ is the "hybridisation width", n_f is the 4f-shell hole occupancy, which is very close to 1 in a weakly hybridised material like $YbAuCu_4$, and Δ_i is the energy of the electronic level from the ground state. We shall consider here only the two exchange split states of the ground Kramers doublet and neglect all excited states. Labelling

n and $\bar{n}$ the occupation numbers of these two states, separated by an energy $\Delta = 2\mu(\Gamma_7)H_{ex}$, it can easily be shown that:

$$\begin{cases} \mu & = \mu(\Gamma_7)\,[n - \bar{n} + 4\varepsilon(n + \bar{n})] \\ \alpha_Q^z & = R(\mathbf{u})A_Q\varepsilon(n - \bar{n}). \end{cases} \tag{11}$$

Introducing an antiferromagnetic molecular field constant $\lambda < 0$, the exchange field is $H_{ex} = \mid \lambda \mid \mu$ and the self consistent equation (11) for μ yields:

$$\mu = \mu(\Gamma_7)(n - \bar{n}) / \left[1 - 4\frac{g_J\mu_B \mid \lambda \mid \mu(\Gamma_7)}{\Delta_8}(n + \bar{n})\right]. \tag{12}$$

As $n - \bar{n} < 1$ and $n + \bar{n} \simeq 1$, these equations show that hybridisation introduces a reduction factor for both the magnetic moment and the E.F.G.. To calculate the moment value, it is necessary to also take into account the effect of exchange enhancement. Estimations indicate that values for $n - \bar{n}$ in the range $0.75 \leq n - \bar{n} \leq 0.8$, $\mid \lambda \mid$ values in the range $0.5\ \mathrm{T}/\mu_B \leq \mid \lambda \mid \leq 1\ \mathrm{T}/\mu_B$, yielding $0.73\ \mathrm{T} \leq H_{ex} \leq 1.46\ \mathrm{T}$, give a good agreement with the experimental μ and α_Q^z values when the exchange field direction is <111> or <110>. The Kondo temperature T_0 can be estimated using the two relations derived from (10):

$$\begin{cases} n - \bar{n} & = \dfrac{\Gamma(1 - n_f)}{\pi} \cdot \dfrac{\Delta}{T_0(T_0 + \Delta)} \\ n + \bar{n} & = \dfrac{\Gamma(1 - n_f)}{\pi} \cdot \dfrac{2T_0 + \Delta}{T_0(T_0 + \Delta)} \end{cases} \tag{13}$$

Introducing the moment reduction ratio $r = \mu/\mu(\Gamma_7)$ and defining T_{RKKY} through: $k_B T_{RKKY} = \mid \lambda \mid \mu(\Gamma_7)^2$, we get, using $n + \bar{n} = n_f \simeq 1$ and taking into account the exchange enhancement (12) of the magnetic moment:

$$\frac{T_0}{T_{RKKY}} = \frac{n_f}{1 - 4\dfrac{g_J\mu_B}{\mu(\Gamma_7)} \cdot \dfrac{T_{RKKY}}{\Delta_8}\, n_f - r} \tag{14}$$

As $T_{RKKY} = (1.60 \pm 0.35)$ K and $r = 0.85$, we obtain for the Kondo temperature: $T_0 = (0.30 \pm 0.10)$ K.

To summarize this section, it can be concluded that the mean values of the hyperfine field and of the induced E.F.G. at $T = 0.05$ K in $YbAuCu_4$ are compatible either with a bare Γ_6 ground state or with a hybridised Γ_7 ground state with a small Kondo temperature $T_0 \simeq 0.3$ K. The derived exchange field in both cases is close to 1T, and its direction is likely to be the <100> axis for the case of a Γ_6 ground state and the <111> or <110> axis for the case of a Γ_7 ground state.

5.2 EFFECT OF STRAINS ON THE MAGNETIC HYPERFINE SPECTRUM. — Small deviations from cubic symmetry of the crystal electric field at a Yb site can be expanded up to second order in **J** using a basis of angular momentum operator-equivalents which transform according to the representations Γ_3 and Γ_5 under the operations of the cubic group. The two Γ_3-like operators are [13]:

$$\begin{cases} O(\Gamma_{3g,\theta}) & = 3J_z^2 - J(J+1) \\ O(\Gamma_{3g,\eta}) & = \dfrac{\sqrt{3}}{2}(J_+^2 + J_-^2), \end{cases} \tag{15}$$

and the three Γ_5-like operators are:

$$O(\Gamma_{5g,i}) = \frac{1}{2}(J_k J_l + J_l J_k), \quad i,k,l = x,y,z \quad \text{and} \quad i \neq k \neq l. \tag{16}$$

A natural choice for the z-axis is one of the high symmetry cubic axes; in the following we present calculations where the z-axis is either the tetragonal <100> axis or the trigonal <111> axis.

The distortion (or strain) Hamiltonian writes therefore:

$$\mathcal{H}_{\text{dis}} = \sum_{i=\theta,\eta} B_{3g,i} O(\Gamma_{3g,i}) + \sum_{i=x,y,z} B_{5g,i} O(\Gamma_{5g,i}). \tag{17}$$

The B coefficients are assumed to be small with respect to the first C.E.F. excitation energy (45 K) which allows $\mathcal{H}_{\text{dis}}$ to be treated in perturbation with respect to the cubic C.E.F. interaction.

To first order perturbation, it turns out that the only term in $\mathcal{H}_{\text{dis}}$ yielding corrections to the magnetic moment is the axially symmetric term $\mathcal{H}_{\text{dis}}^{3g,\theta} = B_{3g,\theta}\left[3J_z^2 - J(J+1)\right]$. This type of distortion is equivalent to an elongation (or compression) of the Yb environment along the local z-axis, i.e. the <100> or <111> axis.

The axial distortion $\mathcal{H}_{\text{dis}}^{3g,\theta}$ has matrix elements between all three states Γ_6, Γ_7 and Γ_8. The first order perturbation parameters will be expressed *via* $\beta = 3B_{3g,\theta}/\Delta_8$ and $\delta = \Delta_8/\Delta_{67} = 0.57$, where Δ_{67} is the energy separation between Γ_6 and Γ_7. Mixing by $\mathcal{H}_{\text{dis}}^{3g,\theta}$ creates an axially symmetric E.F.G. whose principal axis lies along the z-elongation axis. Assuming in a first step that the magnetic moment, i.e. the exchange field, lies along the elongation axis, we obtain the following perturbed values for $\mu = \mu_z$ and α_Q^z :

$$\begin{cases} \mu & = \mu(\Gamma_i)(1 + Q\beta) \\ \alpha_Q^z & = A_Q S\, f(\delta)\beta, \end{cases} \tag{18}$$

where Q and S are numbers depending on the direction of the z-elongation axis and on the type of ground doublet and $f(\delta)$ is a function of the ratio Δ_8/Δ_{67}. Details concerning the calculation of Q, S and $f(\delta)$ are given in Appendix 1. Their values are given in table I.

Table I. — *Coefficients for the first order correction to μ and α_Q^z due to the axial distortion $\mathcal{H}_{\text{dis}}^{3g,\theta}$ (see (18)), when the exchange field is parallel to the strain axis Oz.*

	Γ_6 ground state		Γ_7 ground state	
	$z \,//< 100 >$	$z \,//< 111 >$	$z \,//< 100 >$	$z \,//< 111 >$
Q	-20	$O(\varepsilon^2)$	-4	$-32/3$
S	-210	-70	-18	-128
$f(\delta)$	1	δ	1	$1 + 35/64\delta$

In the general case where the exchange field direction OZ lies at an angle θ from the z-elongation axis, we obtain for the parallel and transverse components of the magnetic moment:

$$\begin{cases} \mu_z & = \mu(\Gamma_i)\cos\theta\left[1 + Q\beta(1 + 1.5\sin^2\theta)\right] \\ \mu_x & = \mu(\Gamma_i)\sin\theta\left[1 - Q\beta\dfrac{1 + 3\cos^2\theta}{2}\right], \end{cases} \tag{19}$$

which gives the magnitude of the moment to first order:

$$\mu = \mu(\Gamma_i)\left[1 + Q\beta\frac{3\cos^2\theta - 1}{2}\right]. \tag{20}$$

The angle θ' between μ and Oz is given by: $\tan\theta' = (1-3Q\beta)\tan\theta$; to first order perturbation, it is equal to θ. The component of the E.F.G. tensor along the hyperfine field direction, i.e the magnetic moment direction, which corresponds to the experimentally measured quadrupolar parameter, writes then:

$$\alpha_Q^Z = \alpha_Q^z\frac{3\cos^2\theta - 1}{2} = A_Q S\ f(\delta)\beta\frac{3\cos^2\theta - 1}{2} \tag{21}$$

Including the exchange field correction obtained in the previous paragraph, we get the complete perturbation expression for the hyperfine field $H_{\rm hf} = C\mu$ and for the Z-component of the E.F.G. for a given strain value (i.e. β value):

$$\begin{cases} H_{\rm hf}(\beta) &= H_{\rm hf}(\Gamma_i)\left[1 + P\varepsilon + Q\beta\dfrac{3\cos^2\theta - 1}{2}\right] \\ \alpha_Q^Z(\beta) &= A_Q\left[R(\mathbf{u})\varepsilon + S\ f(\delta)\beta\dfrac{3\cos^2\theta - 1}{2}\right]. \end{cases} \tag{22}$$

Inspection of expressions (22) leads to the following conclusions:

i) the axial distortion $\mathcal{H}_{\rm dis}^{3g,\theta}$ induces first order corrections to $H_{\rm hf}$ and α_Q^Z if the angle between the exchange field and the elongation axis is different from the "magic angle" $\theta_m = \mathrm{Arcos}(1/\sqrt{3})$.

ii) whatever the angle θ (except θ_m) between the exchange field and the elongation axis on a given site, there exists a linear relationship between $H_{\rm hf}$ and α_Q^Z; for instance, eliminating $\beta\dfrac{3\cos^2\theta - 1}{2}$ between equations (22):

$$\alpha_Q^Z(\beta) = A_Q\frac{S\ f(\delta)}{Q}\left[\frac{H_{\rm hf}(\beta)}{H_{\rm hf}(\Gamma_i)} - 1\right] + A_Q\varepsilon\left[R(\mathbf{u}) - \frac{PS}{Q}f(\delta)\right]. \tag{23}$$

The quantities Q, S and $f(\delta)$ depend only on the direction of the distortion axis whereas the quantity $R(\mathbf{u})$ depends only on the direction of the exchange field.

iii) therefore, in the presence of a distribution of axial strains, i.e. of β values, the resulting distributions of $H_{\rm hf}$ and α_Q^Z values are linearly correlated if the strain axis is the same for all sites, and if the exchange field lies at a fixed angle, different from the "magic angle", with respect to the strain axis. Even for a random orientation of the exchange field, the correlation would still hold in first approximation, but would be slightly smeared by the random values taken by the quantity $R(\mathbf{u})$ which, as is shown below, gives only a small contribution to expression (23).

The experimentally observed significant distribution of hyperfine parameters in $YbAuCu_4$ at $T = 0.05$ K and the linear correlation between them can therefore be interpreted as arising from a distribution of axial C.E.F. distortions of the Yb site along a common symmetry axis; furthermore, the easy magnetisation direction of the antiferromagnetic structure cannot lie at an angle $\theta_m = \mathrm{Arcos}(1/\sqrt{3})$ from the strain axis. This means that if the distortion is along <100>, the magnetic moment direction cannot be <111> and *vice-versa*.

Table II. — *Calculated coefficients of the linear correlation between H_{hf} and α_Q^Z (see (23)) in the presence of axial strains and of an exchange field of 1 T parallel to the strain axis. For the case of a Γ_6 ground state with the z-elongation axis along < 111 >, there is no first order correction to μ and therefore no linear correlation. For the case of a Γ_7 ground state with the z-elongation axis along < 111 >, the pure C.E.F. values and the "hybridised" values are given.*

	Γ_6 ground state		Γ_7 ground state		
	z //< 100 >	z //< 111 >	z //< 100 >	z //< 111 >	
				C.E.F.	hybr.
$A \times 10^2$ (mm/s/T)	2.13	–	0.71	2.48	3.10
B(mm/s)	−2.90	–	−1.24	−4.33	−4.46

In order to compare the coefficients A and B of the linear correlation: $\alpha_Q^Z(\beta) = A\, H_{hf}(\beta) + B$ calculated in (23) with the experimental values, we computed them for the two cases of an elongation axis along <100> or <111>, and in the two hypotheses of a Γ_6 or a Γ_7 ground doublet (see Tab. II). As can be seen on expression (23), the slope A does not depend on the exchange field quantities $\mathbf{u}$ and ε; in contrast, the B coefficient has a contribution: $\varepsilon A_Q \left[R(\mathbf{u}) - \frac{PS}{Q} f(\delta)\right]$ which depends on $\mathbf{H}_{ex}$ for which we know neither its exact magnitude nor its direction. However, this ε-dependant term is small, of the order of $0.1 - 0.2$ mm/s. The numbers given in table II are computed with the assumption that $\mathbf{H}_{ex}$ is 1T and lies along the elongation axis.

We can proceed now with the comparison of the experimental correlation coefficients obtained in section 4.1 (see expression (6)) with the calculated values of table II; all these values are represented in figure 3. For the case of a Γ_6 ground state, the calculated A and B values with the elongation axis along <100> match precisely the experimental values. For the case of a Γ_7 ground state, the calculated correlation with the elongation axis along <100> does not match the experimental data, whereas the A and B values obtained when the elongation axis is along <111> are not far from the experimental correlation. However, we have shown in section 5.1 that, if the ground state is Γ_7, hybridisation must be taken into account. A simple calculation using expressions (11) combined with (18) yields the hybridisation corrected A and B values:

$$\begin{cases} B_{hyb} = \varepsilon A_Q \left[R(\mathbf{u})(n-\bar{n}) - \dfrac{SP\, f(\delta)(n+\bar{n})^2}{Q(n-\bar{n})}\right] - A_Q \dfrac{S\, f(\delta)}{Q}(n+\bar{n}) \\ A_{hyb} = A_Q \dfrac{S\, f(\delta)}{Q\, H_{hf}(\Gamma_i)} \cdot \dfrac{n+\bar{n}}{n-\bar{n}} \end{cases} \tag{24}$$

Using $n + \bar{n} = 1$ and the representative values $n - \bar{n} = 0.8$ and H_{ex}= 1T, we get: $B_{hyb} = -4.6$ mm/s and $A_{hyb} = 3.1 \times 10^{-2}$ mm/s/T, which are very close to experimentally acceptable values (see Fig. 3).

From the measured mean square deviation of the hyperfine field distribution ΔH_{hf}, we can deduce the mean square deviation of the α_Q^Z distribution through relation: $\Delta\alpha_Q^Z = A\, \Delta H_{hf}$, and then obtain the mean square deviation $\Delta B_{3g,\theta}$ of the axial distortion distribution through relation (22). Actually we can only derive the quantity:

$$\Delta B_{3g,\theta} \frac{3\cos^2\theta - 1}{2} = \frac{\Delta H_{hf}}{H_{hf}(\Gamma_i)} \cdot \frac{\Delta_8}{3Q\Delta n} \tag{25}$$

where $\Delta n = 1$ for the case of a Γ_6 ground state without hybridisation and $\Delta n = n - \bar{n} = 0.8$ for the case of a hybridised Γ_7 ground state. For a Γ_6 ground state, we find: $\Delta H_{\rm hf} = 20.5$ T and $\Delta B_{3g,\theta}\dfrac{3\cos^2\theta - 1}{2} = 0.11$ K, and for a Γ_7 ground state: $\Delta H_{\rm hf} = 17$ T and $\Delta B_{3g,\theta}\dfrac{3\cos^2\theta - 1}{2} = 0.17$ K.

5.3 SUMMARY OF RESULTS. — To summarise the results of this section, we can say that the $T = 0.05$ K Mössbauer spectrum in $YbAuCu_4$ shows the existence of a distribution of small strains at the Yb site; in the presence of the exchange field, the spectral shape is sensitive only to axially symmetric distortions. Two hypotheses concerning the Yb^{3+} C.E.F. ground state and the strain axis are compatible with the $T = 0.05$ K experimental data: a Γ_6 ground state with a strain axis along <100>, or a Γ_7 ground state hybridised with band electrons with a strain axis along <111>.

The hypothesis of a Γ_7 C.E.F. ground state is in agreement with the inelastic neutron scattering analysis in $YbAuCu_4$ [9, 10]. In this case, we estimate the hybridisation of the Yb^{3+} ion to correspond to a Kondo temperature $T_0 \simeq 0.3$ K; the magnitude of the exchange field is $H_{\rm ex} = (1.1 \pm 0.35)$T; its direction is not known as the magnetic structure has not been determined, but our data show that the magnetic moment cannot lie along <100> and suggest it could lie along the <111> or the <110> direction. If we assume that the easy magnetisation axis is <111> the mean square deviation of the axial strain distribution is: $\Delta B_{3g,\theta} \simeq 0.17$ K.

6. Mössbauer spectra in the antiferromagnetic phase with applied magnetic field.

6.1 PRELIMINARIES. — When a magnetic field is applied in the antiferromagnetic (AF) phase, Mössbauer spectroscopy on a powder sample can provide information about the orientation of the magnetic moments with respect to the applied field *via* the spectral line intensities. Indeed, due to the rotational properties of the Mössbauer photon which has a well defined angular momentum $l = I_e - I_g$, the intensities of the nuclear transitions depend on the angle θ between the local quantisation axis and the γ-ray propagation direction $\mathbf{k}$. For ^{170}Yb, $l = 2$ and the angular dependencies of the various $\Delta I_z = m$ transitions are:

$$\begin{cases} \Delta I_z(m = \pm 2) &= \dfrac{1}{2}\sin^2\theta(1 + \cos^2\theta) \\ \Delta I_z(m = \pm 1) &= \dfrac{1}{2}(\cos^2\theta + \cos^2 2\theta) \\ \Delta I_z(m = 0) &= \dfrac{3}{4}\sin^2 2\theta \end{cases} \tag{26}$$

In our experimental setup, the magnetic field $\mathbf{H}$ is applied parallel to the $\mathbf{k}$ direction, and the local quantisation axis in the AF phase of $YbAuCu_4$ is the direction of the hyperfine field, i.e. of the Yb^{3+} magnetic moment. For a given ion, the angle θ represents therefore the angle between the directions of the magnetic moment and of the applied magnetic field. In a powder sample in zero applied field, the orientations of the AF moments with respect to the $\mathbf{k}$ direction are at random; as the angular average $\int \Delta I_z(m, \theta)\mathrm{d}\Omega$ is independent of m, all the lines have equal intensities. When a magnetic field is applied, the relative line intensities can depart from unity in the case of a common orientation of the magnetic moments in the whole sample with respect to the field, allowing the angle θ to be measured using expressions (26).

The effect of a magnetic field on an AF structure is well known and depends on the relative strengths of the magnetic anisotropy energy $E_{\rm anis}$ and of the exchange interaction [14]. Two

limiting cases can be singled out: the weak anisotropy case when $E_{anis} \ll \mathcal{H}_{ex}$ and the strong anisotropy case: $E_{anis} \sim \mathcal{H}_{ex}$.

When the magnetic anisotropy is weak, it is easily overcome by a moderate field, resulting in the rotation of the AF structure in each domain perpendicularly to the field direction. This yields a spectrum where the $m = 0$ line is absent ($\theta = \pi/2$). Upon further increase of the field, the two AF sublattices tilt symmetrically towards the field direction until they line up with **H** for a threshold value $H_S = 2H_{ex}$. The spectrum then consists of the two $m = \pm 1$ lines, the $m = 0$ and $m = \pm 2$ lines being absent ($\theta = 0$). The weak anisotropy case is illustrated by our study of the AF phase of the hybridised compound YbAs [6]: a field of 2 T resulted in the rotation of the AF structure and in a slight tilting of the Yb^{3+} magnetic moments, the angle θ being close to 80°. However lining up of the moments along the field direction could not be obtained due to the very high value of the exchange field (7 T) in this compound, compared with the maximum available laboratory field of 5.8 T.

A quite different picture arises when the anisotropy energy is of the same order of magnitude as the exchange energy. Model calculations for the case of an axial anisotropy [14] show that, at low fields, the AF structure does not rotate and that it is not drastically modified. When the applied field is close to parallel to the easy magnetisation axis, the AF configuration is the most stable until the field reaches a threshold value $H_S = H_{ex}$, where a metamagnetic (spin flip) transition occurs towards a ferromagnetic configuration. When the applied field is close to perpendicular to the easy magnetisation axis, the situation is similar to the weak anisotropy case, the threshold field for lining up of the moments being however bigger than $2H_{ex}$. Consequently, at low fields, the powder Mössbauer spectrum is not expected to be very different from a zero field powder spectrum; as the field increases and reaches $H_S = H_{ex}$, a fraction of the magnetic moments should undergo the metamagnetic transition and exhibit a two line spectrum, whose relative weight should increase with further increase of the field as more and more magnetic moments line up along its direction.

6.2 EFFECT OF THE MAGNETIC FIELD ON THE AF STRUCTURE OF $YbAuCu_4$. — We recorded spectra at $T = 0.05$ K in applied fields ranging from 0.2 to 4 T. As can be seen in figure 4, the data suffer from relatively poor signal-to-noise ratio; this is due to the experimental geometrical arrangement, where the distance between the γ-ray source and the $YbAuCu_4$ absorber is quite large because of the presence of the superconducting magnet generating the field. The spectra at 0.2 T, 0.5 T (Fig.4a) and 1 T show no particular line extinction; they are similar to the zero field spectrum (see Fig. 1), the hyperfine field increasing slightly with the applied field but remaining close to the zero field value (Fig.5). The spectral shape suddenly changes for an applied field of 1.5 T: it consists mainly of the two $m = \pm 1$ lines with different widths, the $m = 0$ and $m = \pm 2$ lines being less intense. The spectra at 2 T (Fig.4b) and 3 T are similar to that at 1.5 T, with still decreased intensities of the $m = 0$ and $m = \pm 2$ lines. Fits using the hyperfine Hamiltonian (2) with line intensities given by expressions (26) are satisfactory and yield θ values of 22° for 1.5 T, 20° for 2 T and 15° for 3 T. These angle values must probably be understood as average values because these spectra can also be fitted by a superposition of a powder spectrum (with equal line intensities) and of a two-line ($\theta = 0$) spectrum, the relative intensity of the powder spectrum decreasing with increasing field values. The spectrum at 4 T (Fig.4c) consists of only two lines with different broadenings and is well accounted for using values lower than 10°. Between 1.5 T and 4 T, the energy separation between the two $m = \pm 1$ lines steadily increases, corresponding to an increase of the mean hyperfine field from 173 T to 198 T (see Fig. 5).

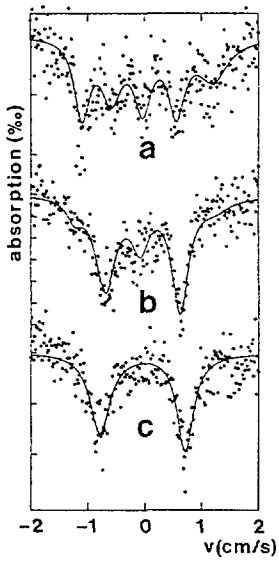

Fig. 4. — ^{170}Yb Mössbauer absorption spectra in $YbAuCu_4$ at $T = 0.05$ K with magnetic field **H** applied parallel to the γ-ray propagation direction. The lines are fits using hyperfine Hamiltonian (2). (a) $H = 0.5$ T; the line intensities are equal (powder spectrum) and the linewidths are fixed at the values obtained in zero field. (b) $H = 2$ T; the line intensities are given by expressions (25) with $\theta = 20°$ and the linewidths are fixed at the values obtained in zero field. (c) $H = 4$ T; the line intensities are given by expressions (25) with $\theta = 0$ and the widths of the two lines are free parameters.

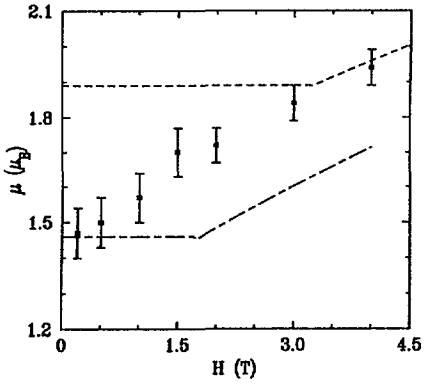

Fig. 5. — Field variation of the magnitude of the Yb^{3+} magnetic moment in the AF phase of $YbAuCu_4$ at $T = 0.05$ K derived from hyperfine field measurements. The squares represent the experimental data. The lines are self-consistent C.E.F. calculations (see text) for a Γ_7 ground state with $\lambda = -0.85T/\mu_B$ (dashed line) and for a Γ_6 ground state with $\lambda = -0.6T/\mu_B$ (dash-dotted line).

6.3 INTERPRETATION. — As we do not observe any extinction of the $m = 0$ line for fields below 1 T, we can conclude that the magnetic AF structure does not reorient perpendicularly to the applied field, evidencing the presence of a sizeable magnetic anisotropy. The predominance

of the two-line spectrum from 1.5 T upwards shows that, for theses field values, an important fraction of the magnetic moments is aligned with the applied field, i.e. that these moments have undergone a metamagnetic-like (spin flip) transition for a threshold field H_S between 1 and 1.5 T. As the field grows, more and more moments line up along its direction; for a field value of 4 T the magnetic structure is ferromagnetic. This metamagnetic behaviour is also characteristic of a strong magnetic anisotropy as outlined in section 6.1. The possible origin of this anisotropy will be discussed in section 8, where it will be tentatively assigned to an exchange anisotropy induced by hybridisation.

The variation of the magnitude of the Yb^{3+} magnetic moment with the applied field, derived from the hyperfine field measurements, is represented in figure 5, together with the field variations of the $T = 0.05$ K moment expected for a Γ_6 and a Γ_7 ground state supposed hybridisation free. The moment is calculated in the simplest case of weak anisotropy: it remains saturated up to the spin-flip field $H_S \simeq 2H_{ex}$, and then it is computed self-consistently using the molecular field constant determined in section 5, and starting from an appropriate cubic C.E.F. level scheme described by the x and W parameters [15]. For the case of a Γ_7 ground state, we use $x = -0.945$ and $W = -2.61$ K as determined in reference [9]. For the case of a Γ_6 ground state, we use $x = 0.85$ and $W = -2.86$ K which yield the same energy separations between levels as observed in reference [9]. It is to be noticed that the quasi-linear increase of the moment with the field for $H > H_S$ is due solely to quantum mixing and that the slope writes, to first order perturbation, and with the notations of section 5: $\mu(\Gamma_i)Pg_J\mu_B/\Delta_8$, i.e. it does not depend on the molecular field constant λ. As the field increases, the magnitude of the moment departs from the Γ_6 curve and, from 3 T upwards, is correctly accounted for by the Γ_7 curve with λ values in the upper end of the range determined in section 5: $-1\text{T}/\mu_B \leq \lambda \leq -0.7\text{T}/\mu_B$. We interpret this behaviour in the following way: the C.E.F. ground state of Yb^{3+} in $YbAuCu_4$ is the Γ_7 doublet and the field variation of the magnitude of the moment reflects the crossover from a hybridisation reduced value at low fields towards a pure C.E.F. value at high fields. Indeed, the effects of hybridisation are expected to be suppressed by fields greater than a critical field $H_K \sim k_B T_0/\mu$. Using the estimation $T_0 \simeq 0.3$ K obtained in section 5, we get: $H_K \sim 0.4$T; therefore, for magnetic fields $H \gg H_K$, the Yb^{3+} magnetic moment should recover its C.E.F. value, what is experimentally observed.

6.4 SUMMARY. — The Mössbauer data with an applied field in the AF phase of $YbAuCu_4$ allow us to discard one of the hypotheses put forward in section 5: the Yb^{3+} C.E.F. ground state cannot be the Γ_6 doublet; it is the Γ_7 doublet weakly hybridised with conduction electrons, in agreement with reference [9]. A sizeable magnetic anisotropy is evidenced which leads to a metamagnetic-like behaviour of the magnetic structure. The threshold field for spin flip, which is expected to be $H_S \simeq H_{ex}$, is found to lie in the range $1\text{ T} \leq H_S \leq 1.5$ T; this is consistent with the derived mean value of the molecular field constant $\lambda = -0.85\text{T}/\mu_B$ (Sect. 5.1), which yields $H_{ex} = 1.25$ T.

7. Mössbauer spectra and magnetic measurements in the paramagnetic phase.

This section presents the experimental results and their interpretation at temperatures $T \geq 4.2$ K. In this temperature range, the effects of hybridisation associated with a Kondo temperature $T_0 \simeq 0.3$ K are expected to be weak, at least as concerns the magnetic moment and E.F.G. values. This is confirmed by our calculations using the model of reference [11]. Therefore, in this section, interpretation of the data neglects hybridisation and starts from the cubic C.E.F. level scheme of reference [9] with a Γ_7 ground state ($x = -0.945$ and $W = -2.61$ K). The

z-axis of the $\mathcal{H}_{3g,\theta}$ strains is therefore assumed to be the <111> direction. The full C.E.F. Hamiltonian writes:

$$\mathcal{H}_{\text{C.E.F.}} = \mathcal{H}_{\text{cub}}(x, W) + B_{3g,\theta}\left[3J_z^2 - J(J+1)\right]. \tag{27}$$

For the data in the presence of a large magnetic field, the Zeeman interaction is included and the complete Hamiltonian is diagonalised. Furthermore, in this temperature range where $T > 4\,T_N$ and for applied field values $H \geq 4$ T, much higher than the estimated anisotropy field (≤ 1.5 T, see Sect. 6), the anisotropy of the interionic exchange coupling will be neglected. Exchange is self-consistently taken into account *via* an antiferromagnetic molecular field constant λ which, in the paramagnetic phase, reduces the magnetic moment (or hyperfine field) value with respect to the pure C.E.F. value.

7.1 MÖSSBAUER SPECTRA IN ZERO APPLIED FIELD. — In the paramagnetic phase (above 1.2 K) the main component of the spectra is a single line whose width gently decreases from 6.2 mm/s at $T = 4.2$ K to 4.3 mm/s at 60 K. On the spectra at $T = 4.2$ K (see Fig.6) and 10 K, a second component is visible, which consists of a split spectrum and amounts to $10 - 15$ % of the whole spectral intensity. This spectrum can be accounted for by an axial quadrupolar hyperfine interaction:

$$\mathcal{H}_Q = \alpha_Q(I_z^2 - 2) \tag{28}$$

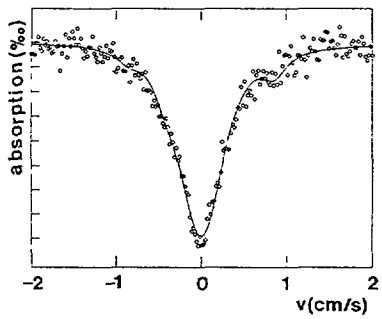

Fig. 6. — ^{170}Yb Mössbauer absorption spectrum in $YbAuCu_4$ at $T = 4.2$ K. The line is a two-component fit: the central broad line (85 %) corresponds to a Gaussian distribution of axial strains with $\langle B_{3g,\theta}\rangle = 0$ and $\Delta B_{3g,\theta} = 0.37$ K and the other component (15 %) is an axial quadrupolar spectrum with $\alpha_Q = 4.3$ mm/s (see text).

where $\alpha_Q = \dfrac{eQV_{zz}}{8}$, the z-axis being the principal axis of the E.F.G. tensor. The rather high obtained values: $\alpha_Q(4.2\text{ K}) = 4.3$ mm/s and $\alpha_Q(10\text{ K}) = 3.3$ mm/s show that these Yb ions lie at sites with non-cubic symmetry. As the impurity content of our sample is quite low, we think these sites pertain to the $YbAuCu_4$ phase and that they are associated with stoichiometry defects (see discussion in Sect. 8). Such defects can create sizeable distortions from cubic symmetry and therefore, significant alterations of the ground wave-functions. Indeed, the above mentioned α_Q values are actually close to those associated with an electronic state arising in the presence of a dominant axial C.E.F. component. In the magnetically ordered

phase, these Yb ions should give rise to non-cubic hyperfine field spectra but their contributions are not resolved from the main spectrum analysed in section 5.

The majority of the Yb ions, which yield the broadened single line-spectrum, lie at sites with cubic or quasi-cubic symmetry. The broadening can be due to dynamical effects (paramagnetic relaxation) and/or to the distribution of small distortions of the Yb site evidenced in the $T = 0.05$ K spectrum. The latter indeed lead to a distribution of small electric field gradients at the Yb site and the resulting spectrum is a superposition of unresolved quadrupolar hyperfine spectra yielding a single broad line. The paramagnetic relaxation rate $1/T_1$ within the ground doublet can be estimated (at temperatures well below the C.E.F. excitation energy) by the half-width of the quasi-elastic line of the neutron inelastic spectra. Following the analysis of reference [9], one finds: $1/T_1(4.2\ \text{K}) \simeq 40$ GHz and $1/T_1(10\ \text{K}) \simeq 60$ GHz. The relaxation frequency is therefore much greater than the magnetic hyperfine constant A of the ^{170}Yb isotope associated with the Γ_7 doublet: $A(\Gamma_7) \simeq 0.9$ GHz [12]. In this "quasi-rapid" relaxation regime, the dynamical broadening of the Mössbauer line is given by (see Appendix 2):

$$\Delta\Gamma_R = 3A(\Gamma_7)^2 T_1. \tag{29}$$

Using the above values of $1/T_1$, one obtains, at $T = 4.2$ K : $\Delta\Gamma_R = 0.8$ mm/s. As the overall linewidth at $T = 4.2$ K is 6.2 mm/s, static effects are therefore dominant in building up the line broadening.

In the absence of a polarising (magnetic or exchange) field, both the Γ_3-like and Γ_5-like strains yield first order contributions to the E.F.G. tensor. However, we shall give here an analysis of the static broadening of the main component of the paramagnetic spectra assuming that the only strain present is that evidenced in the AF phase, i.e. $\mathcal{H}_{3g,\theta}$ along the <111> axis. The analysis of the spectra at T=4.2K with high magnetic fields shows that this assumption is very likely (see Sect. 7.2). So, starting from Hamiltonian (27), we calculate the Boltzmann average of the E.F.G. tensor over the C.E.F. levels for a given $B_{3g,\theta}$ value, which yields the quadrupolar parameter α_Q in the rapid or quasi-rapid relaxation regime. The final spectrum is obtained by introducing a Gaussian shaped distribution of the strain parameter $B_{3g,\theta}$ and by assigning a width $G = 2.7$ mm/s + $\Delta\Gamma_R$ to each elementary spectrum. The lineshape then depends only on the centroid $\langle B_{3g,\theta}\rangle$ and on the mean square deviation $\Delta B_{3g,\theta}$ of the distribution. At $T = 4.2$ K (see Fig. 6) and 10 K, the presence of the extra spectrum arising from Yb ions in non-cubic sites somewhat hinders a precise determination of the distribution parameters to be done. Nevertheless, the spectra at these two temperatures can be coherently fitted using the following values: $|\langle B_{3g,\theta}\rangle| < 0.1$ K and $\Delta B_{3g,\theta} = (0.37 \pm 0.07)$ K. At higher temperature, the spectra are correctly accounted for using the above parameters, which means that the decrease of the spectral width from 4.2 K to 60 K is due for a small part to the decrease of the dynamical broadening and mainly to the Boltzmann averaging of the E.F.G. tensor as temperature increases.

With the assumption that only axial strains are present in $YbAuCu_4$, we can conclude that their distribution has a Gaussian shape and is symmetrical with respect to zero to a good approximation, i.e. that there is no average distortion of the cubic Yb site over the sample: $\langle B_{3g,\theta}\rangle = 0$. We can also combine the value of $\Delta B_{3g,\theta}$ determined here and the result of section 5 to obtain the angular factor of expression (25); we find: $\dfrac{3\cos^2\theta - 1}{2} \simeq 0.5$, or $\theta \simeq 35°$. As the strain axis is the <111> axis, this suggests that the direction of the exchange field, and therefore of the magnetic moment, in the AF phase is the <110> axis.

7.2 MÖSSBAUER SPECTRA WITH APPLIED MAGNETIC FIELD AT $T = 4.2$ K. — In presence of a magnetic field H, the direction of the induced magnetic moment on each paramagnetic Yb

ion is determined by the relative strengths and directions of the single ion C.E.F. anisotropy, of the exchange anisotropy (neglected here) and of the Zeeman interaction. Then, for the majority of the Yb ions, which lie at sites with quasi-cubic symmetry, the induced magnetic moment is expected to lie close to parallel to H due to the weak crystalline anisotropy of the cubic wave-functions. The angle between the hyperfine field and the k direction is therefore close to zero for these ions, yielding a spectrum where the $m = \pm 2$ and $m = 0$ transitions have very small intensities. The spectra at 4.2 K under 4 T and 7 T (see Fig. 7) can indeed be interpreted as arising mainly from these quasi-cubic Yb ions: they consist of two well separated lines corresponding to the $m = \pm 1$ transitions, the $m = 1$ (left side) line being substantially broader than the $m = -1$ line. An extra absorption is visible near the center of the spectrum, which amounts to about 15 % of the total absorption; we think it originates in those Yb ions at sites with non-cubic symmetry which were evidenced in the spectra with zero applied field. For these ions the C.E.F. anisotropy is important and the induced magnetic moment is not expected to lie close to the applied magnetic field, yielding spectra with no particular line extinctions and therefore with possibly a substantial central spectral contribution. In the following, we shall restrict ourselves to the analysis of the majority quasi-cubic spectral contribution; for this purpose, the fits were performed without taking account of the central part of the spectra.

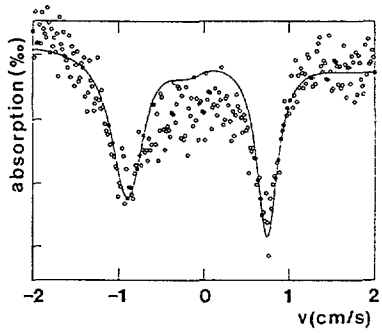

Fig. 7. — ^{170}Yb Mössbauer absorption spectrum in $YbAuCu_4$ at $T = 4.2$ K with a magnetic field of 7 T applied parallel to the γ-ray propagation direction. The solid line is a fit corresponding to a Gaussian distribution of axial strains with $\langle B_{3g,\theta} \rangle = 0$ and $\Delta B_{3g,\theta} = 0.37$ K (see text).

In a first step, the spectra are fitted to the hyperfine Hamiltonian (2) with line intensities given by expressions (26) where the angle θ is zero. The following hyperfine parameters were obtained: for $H = 4$T, $H_{\rm hf} = (157.5 \pm 5)$T and $\alpha_Q^Z \simeq 0.5$ mm/s, and for $H = 7$ T, $H_{\rm hf} = (209 \pm 5)$T and $\alpha_Q^Z \simeq 1$ mm/s. In the present case where the Zeeman interaction cannot be considered as a perturbation with respect to the C.E.F. interaction, a small anisotropy results for the induced magnetic moment, and hence for the hyperfine field, by mixing of the ground doublet with the anisotropic Γ_8 quartet. This implies that both hyperfine field and E.F.G. tensor depend on the orientation of the field with respect to the cubic axes. As the local axes are at random with respect to the field, this results in a small distribution of hyperfine parameters and yields a two-line spectrum with small line-broadenings. The fitted values for $H_{\rm hf}$ and α_Q^Z have then to be considered as average values.

In a second step, we calculate the spectra starting from the cubic C.E.F. alone to which is added the Zeeman interaction. We find that the line positions are correctly accounted for if we

allow for a non-zero molecular field constant; for $H = 4$ T we get: $\lambda = -(0.5 \pm 0.2)\mathrm{T}/\mu_\mathrm{B}$ and for $H = 7$ T : $\lambda = -(0.8 \pm 0.2)\mathrm{T}/\mu_\mathrm{B}$, i.e. an average value of $-0.7\mathrm{T}/\mu_\mathrm{B}$ which is in good agreement with that deduced from the spectra in the AF phase (Sects. 5 and 6.3). In this approach, the $m = 1$ line is slightly broader than the $m = -1$ line, but this "anisotropy" broadening is much smaller than the experimental broadening which is caused by the distribution of C.E.F. distortions, as is shown below.

The third step in our analysis of the spectra with applied magnetic field consists in introducing the distribution of distortions evidenced earlier in order to account for the line broadenings. This assumption, i.e. that the broadenings are of static origin (due to a distribution of local strains), is justified since the dynamical broadening $\Delta\Gamma_\mathrm{R}$ of the $m = \pm 1$ lines in the presence of a magnetic field is very small in the rapid relaxation regime $1/T_1 \gg A(\Gamma_i)$. Indeed, in that case, $\Delta\Gamma_\mathrm{R}$ can be shown to be the same for both lines and to be given by the expression (see Appendix 2):

$$\Delta\Gamma_\mathrm{R} = \frac{1}{2} A(\Gamma_i)^2 T_1 \left[1 - \mathrm{th}^2 \frac{\Delta}{2k_\mathrm{B}T}\right] \tag{30}$$

where Δ is the Zeeman energy separation of the ground doublet. At $T = 4.2$ K with $1/T_1 \simeq 40$ GHz, we get $\Delta\Gamma_\mathrm{R}(4\ \mathrm{T}) = 0.05$ mm/s and $\Delta\Gamma_\mathrm{R}(7\ \mathrm{T}) = 0.012$ mm/s which are negligible with respect to the line width which lies in the range $4 - 5$ mm/s. For the same reason as explained in section 5, in the presence of a magnetic field the axial distortion $\mathcal{H}_{3g,\theta}$ alone contributes to the spectral shape to first order perturbation. Thus, starting from Hamiltonian (27) to which is added the Zeeman interaction, we calculate the rapid relaxation spectrum in the presence of a Gaussian shaped distribution of the $B_{3g,\theta}$ parameter, assigning the minimal experimental linewidth $G = 2.7$ mm/s to each subspectrum. In contrast with the situation in the AF phase, the angle between the hyperfine field and the crystal axes is not the same throughout the sample but is at random because, in the paramagnetic phase, the hyperfine field lies close to the applied magnetic field. Therefore an angular average has to be performed and the spectral shape depends on the mean square deviation $\Delta B_{3g,\theta}$ alone and not on a product of the type $\Delta B_{3g,\theta} \cdot \dfrac{3\cos^2\theta - 1}{2}$ as in the AF phase. These spectra thus provide a direct measurement of the mean square deviation of the axial C.E.F. strains. Using $\lambda = -0.7\mathrm{T}/\mu_\mathrm{B}$, we find that the broadenings and positions of the two lines are correctly reproduced for the two field values by using the same axial strain distribution as derived by fitting of the zero field $T = 4.2$ K spectrum (Sect. 7.1): $\langle B_{3g,\theta}\rangle = 0$ and $\Delta B_{3g,\theta} = (0.37 \pm 0.07)$ K (see Fig. 7). The central absorption is of course not accounted for in this type of fit. This shows that the assumption made in fitting the zero field spectrum, i.e. that the axial strains are the dominant origin of the broadening in $YbAuCu_4$, is correct. If other types of distortions were present, it would not be possible to account both for spectra with and without applied field with the same distribution of axial $B_{3g,\theta}$ parameters.

7.3 MAGNETISATION AND MAGNETIC SUSCEPTIBILITY MEASUREMENTS. — The magnetisation curve $\mu(H)$ of our $YbAuCu_4$ sample at $T = 4.2$ K is shown in figure 8 (black dots). It is linear below 2 T and shows no saturation up to 4.6 T. Also represented are the values of the mean magnetic moment deduced from the Mössbauer spectra at 4 and 7 T (open squares); for cubic symmetry, these values should be very close to those obtained by a direct magnetisation measurement. In order to calculate the powder Yb^{3+} magnetisation, we neglected the distribution of small axial strains. Indeed, it is symmetric with respect to zero and therefore does not modify the average magnetisation with respect to the cubic value in the linear regime (for fields below 1.5 T); at higher fields, our calculations show that the deviation from the cubic value is very small for a distribution with a mean square deviation of the order of 0.5 K. When

comparing the calculations with experiment, we have to bear in mind that around 15 % of the Yb ions lie at sites with non-cubic symmetry. As shown in figure 8, the magnetisation curve for $H < 4.6$ T is correctly accounted for with a molecular field constant $\lambda = -0.5$ T/μ_B; to account for the moment value at 7 T however, a different value $\lambda \simeq -0.85$ T/μ_B is required as determined from the Mössbauer spectrum. This discrepancy could be due to the presence of the non-cubic Yb ions (15 %); trial calculations assuming a strongly anisotropic g-tensor for these ions show that the sample magnetisation, taking into account this non-cubic contribution, departs from the cubic curve in the following way: it lies slightly above the cubic values for fields below about 4 T and slightly below for larger fields. This effect could explain the fact that the low field part of the $\mu(H)$ curve of the sample is accounted for, with a cubic C.E.F. level scheme, using a smaller λ than for the high field point. The fact that the two curves cross for a field of about 4 T would explain why the Mössbauer derived value at 4 T, which represents a cubic only value, coincides with the magnetisation measurement, which is an average over the sample and therefore includes the non-cubic contribution. Using the intermediate value $\lambda = -0.7$ T/μ_B, the cubic only Mössbauer derived magnetic moments at 4 and 7 T are reproduced approximately; this slight disagreement could arise from the fact that we neglected both the anisotropy of the exchange and the strain distribution in the calculation.

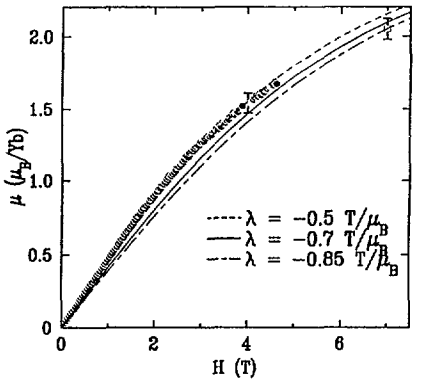

Fig. 8. — Magnetisation *versus* magnetic field in $YbAuCu_4$ at $T = 4.2$ K. (•): experimental data; (□): magnetisation values derived from the Mössbauer spectra with fields of 4 and 7 T; lines: calculations from the C.E.F. level scheme of reference [9] with different molecular field constants: $\lambda = -0.5\text{T}/\mu_B$ (- - - - - -), $\lambda = -0.7\text{T}/\mu_B$ (————) and $\lambda = -0.85\text{T}/\mu_B$ (— - — -).

The comparison between the magnetic moment values derived from a purely magnetic measurement and from a hyperfine field measurement can provide us with an order of magnitude of the conduction electron polarisation contribution to the hyperfine field. This contribution is difficult to evaluate; it is expected to be proportional to the magnetic (or exchange) field. For $H = 4$ T and at $T = 4.2$ K, the magnetisation per Yb^{3+} ion is: $\mu(4\text{ T}) = (1.54 \pm 0.03)\mu_B$. This would yield a 4f electron contribution to the hyperfine field: $H_{hf}^{4f}(4\text{ T}) = (157 \pm 4)$ T. This value is very close to the experimental value of the hyperfine field for $H = 4$ T and at $T = 4.2$ K : $H_{hf} = (157.5 \pm 5)$ T; the conduction electron contribution to H_{hf} must therefore be very small for $H = 4$ T and not greater than a few 1 T. In the magnetically ordered phase, where $H_{ex} \simeq 1$ T (see Sect. 4), the conduction electron contribution to the hyperfine field is negligible.

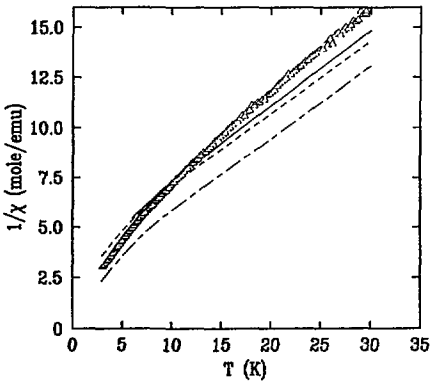

Fig. 9. — Inverse of the magnetic susceptibility *versus* temperature for $H = 136$Oe in $YbAuCu_4$. (Δ): experimental data; lines: calculations from the C.E.F. level scheme of reference [9] with different assumptions: cubic C.E.F. (— - — -), cubic C.E.F. with a molecular field constant $\lambda = -0.7\mathrm{T}/\mu_B$ (- - - - - - -), and cubic C.E.F. with $\lambda = -0.7\mathrm{T}/\mu_B$ and with a Gaussian distribution of axial strains of mean square deviation $\Delta B_{3g,\theta} = 0.37$ K (————).

The inverse magnetic susceptibility of our $YbAuCu_4$ sample between 3 K and 30 K is represented in figure 9. Between 15 K and 30 K, it can be accounted for by a Curie-Weiss type law $1/\chi \propto (T + \theta)$, with $\theta \simeq -8.5$ K. The calculated curve using the cubic C.E.F. only, shown as the dash-dotted line on figure 9, lies significantly below the experimental data. Introducing the molecular field constant $\lambda = -0.7$ T$/\mu_B$ yields a curve closer to experiment (dashed line); taking into account the distribution of axial strains along the <111> direction with mean square deviation $\Delta B_{3g,\theta} = 0.37$ K (solid line) further improves the agreement with experiment but does not reproduce the data exactly. The discrepancy is probably due here again to the presence of the Yb ions at non-cubic sites.

7.4 SUMMARY. — The Mössbauer data in the paramagnetic phase of $YbAuCu_4$ reveal the presence of a fraction (15 %) of Yb ions lying at sites with non-cubic symmetry, which very likely pertain to the $YbAuCu_4$ phase and are close to a stoichiometry defect (see discussion in Sect. 8). Analysis of the majority quasi-cubic spectral contribution suggests that the dominant strains at the Yb site are axial with $O(\Gamma_{3g,\theta})$ type. Their axis is the <111> direction and their distribution, which has approximately Gaussian shape, is symmetrical with respect to zero and has a mean square deviation of about 0.37 K. This would imply that the direction of the spontaneous Yb^{3+} magnetic moment in the AF phase is the <110> direction. The interpretation of both Mössbauer data and magnetic measurements requires the presence of an mean antiferromagnetic molecular field constant of about -0.7 T$/\mu_B$ which is in reasonable agreement with the λ value derived from the measurements in the AF phase.

8. Discussion of the results.

8.1 STRUCTURAL PROPERTIES. — Comparison of the lattice parameters of the $YbXCu_4$ compounds (X = Ag, Au, Pd) prepared by different authors [7, 9, 10, 16, 17] and by us shows an important variability that probably originates in the details of the fabrication procedure to which these compounds seem to be very sensitive. The dependance of the cubic lattice

parameter upon Yb content has been measured in the $YbAgCu_4$ compound [17]: it was found that it decreases as the Yb content increases. Our $YbAuCu_4$ sample shows a sizeable dispersion of cubic lattice parameters reflected in the rather large width of the x-ray diffraction lines at high angles. As the Yb stoichiometry is not very precisely monitored in these compounds we assign this dispersion mainly to an inhomogeneous Yb composition. It could be due, as mentioned in section 2, to the repeated number of meltings that were required to prepare 50 g of the alloy, from which 2g were extracted for the Mössbauer measurements. To a lesser extent, inhomogeneities in the Au and Cu concentrations, or substitutional disorder between Au and Cu atoms could contribute to the parameter dispersion.

On a microscopic scale, the Mössbauer data reveal the presence of 15 % of Yb ions lying at sites where cubic symmetry has been destroyed. These sites therefore suffer from a strong perturbation of their neighbouring environment. The nearest and next-nearest neighbours of a Yb ion in the C15b structure are Cu and Au atoms, among which some disorder can occur; however, we think that substitution of a metallic cation by another cannot create a big perturbation of the cubic C.E.F. because Cu and Au both have one valence electron. In contrast, the presence of a nearest neighbour Yb vacancy (or substitution by a metallic cation) is expected to generate a localised charge defect which induces a strong C.E.F. perturbation. As each Yb^{3+} ion has 8 Yb^{3+} nearest neighbours, a 2 % Yb deficiency creates 16 % strongly non-cubic Yb sites. As the 6 next nearest Yb neighbours would also be affected (to a lesser extent), the presence of 15 % non-cubic Yb sites in our sample can be accounted for by an overall Yb vacancy level of about 1 %.

Besides these highly perturbed Yb sites, the majority of Yb ions lie at basically cubic sites experiencing a small non-cubic C.E.F. component, corresponding mainly to an axial strain along a <111> axis. These strains show a distribution of approximately Gaussian shape, with a mean square deviation $\Delta B_{3g,\theta} \simeq 0.4$ K and with zero mean value over the sample. This distribution is very sensitive to the preparation procedure: in an arc melted $YbAuCu_4$ sample [16] the Mössbauer spectrum at $T = 4.2$ K shows that the mean square deviation of the strain distribution is 60 % greater than in our sample. This sample has a lattice parameter of 7.048(3) Å and contains 21 % of Yb ions at non- cubic sites, which is in rough agreement with an estimated Yb stoichiometry of 0.98. In line with the discussion in the preceeding paragraph, we think these small strains arise from perturbations within the Cu and Au sublattices (probably mainly disorder) which are not expected to significantly alter the cubic symmetry of the Yb site. It can be noted that the Au atoms in the C15b structure are located on <111> axes if the origin is chosen at a nearest neighbour Yb ion: this fact could be related to the predominance of axial strains along <111> in the case where the crystallographic defects would involve mainly the Au atoms.

Another explanation for this strain distribution which preserves the overall cubic symmetry can be put forward: it could arise from a random elongation or compression along the <111> directions of the metallic "cage" surrounding a Yb atom. The coefficient $B_{3g,\theta}$ is the product of a magneto-elastic constant $V(\Gamma_3)$ and of a relative deformation $\varepsilon_{3g,\theta}$ [13, 18]; the order of magnitude of $\varepsilon_{3g,\theta}$ is a few 10^{-3} and $V(\Gamma_3)$ can reach a few 10 K, yielding a mean square deviation $\Delta B_{3g,\theta}$ of a few 0.01 K as was found in rare earth dilute alloys by E.P.R. [18] and Mössbauer spectroscopy [19]. As $\Delta B_{3g,\theta}$ in $YbAuCu_4$ is bigger by one order of magnitude, we think the strains in this material are predominantly caused by structural defects and not by a random Jahn-Teller like mechanism that would distort the "molecule" formed by the 12 Cu atoms and the 4 Au atoms nearest neighbours of a Yb atom.

Therefore, we tentatively relate the distribution of lattice parameters and the presence of non-cubic Yb sites to Yb deficiencies: our sample would then Yb richer than the arc melted sample because its mean lattice parameter is smaller (7.040 Å *versus* 7.048 Å) and because it

contains less non-cubic Yb sites (15 % *versus* 21 %). As to the distribution of small strains it probably arises from substitutional defects which we relate to local inhomogeneities of the Au and Cu environment; in that sense, our sample appears to be more stoichiometric than the arc melted sample [16].

8.2 THE Γ_8 QUARTET AS THE Yb^{3+} GROUND STATE IN $YbAuCu_4$. — Although the inelastic neutron scattering study [9] assign Γ_7 as the C.E.F. ground state of Yb^{3+} in $YbAuCu_4$, it is of interest to check whether the Mössbauer data and the magnetic measurements allow one to rule out the possibility of the Γ_8 quartet as the C.E.F. ground state. The cubic C.E.F. can be chosen so as to yield a Γ_8 ground state and the excited doublets both at an energy of about 45 K from the ground state, in order to be compatible with the neutron spectra: this is achieved using the parameters $x = 0.38$ and $W = -2$ K.

Then, it turns out that the magnetisation and Mössbauer measurements in the paramagnetic phase, in the presence or the absence of an applied magnetic field, are not selective to distinguish between the two C.E.F. level schemes. In the limit of experimental uncertainties, these data can be reproduced consistently with the two kinds of level schemes using comparable molecular field and strain parameters.The situation is different for the spectra in the AF phase in zero field. Indeed, the $T = 0.05$ K Mössbauer spectrum can be rather satisfactorily reproduced in the hypothesis of a Γ_8 ground state with the following parameters: an exchange field of 0.08 T parallel to the <111> direction and axial strains along <100> with a mean square deviation of 0.01 K. However, the magnetic energy involved is small, of the order of 0.16 K, much lower than the transition temperature $T_N = 1$ K; this does not allow the thermal dependence of the spectra in the AF phase to be reproduced. Furthermore, the magnitude of the axial strains (0.01 K) is much too small to account for the width of the $T = 4.2$ K spectrum with a large magnetic field.

Therefore, the possibility of a Γ_8 ground state for Yb^{3+} in $YbAuCu_4$ can be ruled out unambiguously.

8.3 HYBRYDISATION AND INTERIONIC INTERACTION. — To obtain the Kondo temperature of Yb^{3+} in $YbAuCu_4$, we used the variational expressions of the hybridised level occupancies at $T = 0$ K given in reference [11], and applied them to analyse the $T = 0.05$ K data. In this analytical approximate calculation (see Sect. 5.1), we neglected the excited C.E.F. states and the small hole occupancy $1 - n_f$ of the 4f shell induced by hybridisation, as well as the effect of temperature which could be sizeable because the derived T_0 value is small. In order to check the validity of these approximations, we performed the complete finite temperature calculation using the model of reference [11] and the cubic C.E.F. level scheme of reference [9] for various values of the exchange field and of T_0. Agreement between the calculated and experimental values of the spontaneous Yb^{3+} magnetic moment at $T = 0.05$ K is obtained, with a bare hybridisation width $\Gamma = 1$ meV, for similar T_0 values as determined earlier: $T_0 = (0.3 \pm 0.15)$ K. The 4f occupancy is found to lie in the range: $0.94 \leq n_f \leq 0.98$, i.e. the departure from trivalency is very small.

The measured value of the interionic exchange coupling T_{RKKY} (defined as $k_B T_{RKKY} = | \lambda | \mu (\Gamma_7)^2$) is about 1.6 K; it is greater than T_0 and therefore magnetic ordering is expected to occur according to Doniach's modelisation [3] of the interplay between hybridisation and RKKY interaction. The effect of the Kondo spin fluctuations on the characteristics of the magnetic phase are modest in $YbAuCu_4$: the effective ordering temperature is somewhat smaller than the strength of the RKKY interaction ($T_N < T_{RKKY}$) and the reduction of the spontaneous Yb^{3+} magnetic moment with respect to the expected C.E.F. value is 20 %. Another possible consequence of the presence of hybridisation, i.e. the anisotropy of the

exchange coupling, is discussed below.

The Kondo temperature of Yb^{3+} in $YbAuCu_4$ is therefore very much lower than in the isoelectronic non-magnetic Kondo lattice $YbAgCu_4$ (T_0 = 110 K); the 4f brehmsstrahlung isochromat spectra of $YbAgCu_4$ and $YbAuCu_4$ reported in reference [20], which reflect the one-electron density of states above the Fermi energy E_F, seem to show a Kondo resonance at E_F in both compounds, with a larger weight in $YbAgCu_4$ that could account for the larger T_0 in this compound.

8.4 ANISOTROPY OF THE INTERIONIC EXCHANGE INTERACTION. — The anisotropy of the exchange interaction in the AF phase of $YbAuCu_4$ was evidenced by application of a magnetic field on the powder sample; it was found that the magnetic moments remain pinned to their easy magnetisation axis upto fields of 1.5 T, which is of the order of magnitude of the exchange field. This indicates that the anisotropy energy is not small with respect to the exchange energy. The origin of this anisotropy lies with the crystal field interaction or with the exchange interaction itself. For cubic symmetry the crystalline anisotropy is expected to be quite small. In $YbAuCu_4$, the axial strains evidenced at the Yb site, described by the operator $B_{3g,\theta}\left[3J_z^2 - J(J+1)\right]$, correspond to an anisotropy energy:

$$E_{\text{anis}}(\theta) = \frac{-3\mu(\Gamma_i)H_{ex}QB_{3g,\theta}}{\Delta_8} \cdot \frac{3\cos^2\theta - 1}{2} \tag{31}$$

with the notations of section 5. This defines an easy magnetisation axis which is along the strain axis if $B_{3g,\theta}$ is negative and perpendicular to the strain axis if $B_{3g,\theta}$ is positive. However, within a given crystallite, the $B_{3g,\theta}$ values are distributed symmetrically with respect to zero and the strain axes very probably randomly occupy the <111> axes; furthermore the ratio $\frac{E_{\text{anis}}(\theta)}{k_B T_{\text{RKKY}}}$, according to expression (31), is of the order of magnitude of $B_{3g,\theta}/\Delta_8$, i.e. much smaller than unity. Therefore, a bulk easy magnetisation axis cannot be defined by this mechanism and the observed anisotropic behaviour in $YbAuCu_4$ does not arise from C.E.F. distortional effects, but is likely to originate in the interionic exchange coupling.

The interionic interaction in the presence of hybridisation is mediated by the Coqblin-Schrieffer coupling [4] between the 4f electrons and the conduction electrons. The two-ion coupling was shown to be anisotropic with respect to the interionic axis and was invoked to explain the magnetic structures and magnetic anisotropy observed in the cubic Ce monopnictides [21]. The calculation made for Ce^{3+} in reference [21] starts from the free ion states $|J = 5/2, J_z = m\rangle$, which are assumed to be the eigenstates of the Ce^{3+} ion in the material. This approach is valid if the interionic interaction overcomes the C.E.F. interaction, which seems to be the case in some of the Ce monopnictides. In $YbAuCu_4$ however, the ground state is the Γ_7 cubic doublet, and it would be of interest to perform an anisotropy calculation similar to that of reference [21] for the cubic case. Nevertheless we tentatively attribute the observed exchange anisotropy in $YbAuCu_4$ to the presence of hybridisation between 4f electrons and band electrons.

9. Conclusion and summary.

We performed ^{170}Yb Mössbauer and magnetic measurements in the cubic heavy electron material $YbAuCu_4$ at low temperature. A transition to an antiferromagnetic phase is found at T_N = 1 K in our sample, while the transition temperature previously reported for this compound is 0.6 K [7]. We confirmed that the Crystal Electric Field ground state of the Yb^{3+} ion

is the Γ_7 doublet, in agreement with an inelastic neutron scattering study [9]. In the antiferromagnetic phase, we measured a 20 % reduction of the saturated Yb^{3+} magnetic moment with respect to the Γ_7 value, and we evidenced the presence of a sizeable exchange anisotropy. We attribute these two features to hybridisation of the Yb 4f electrons with band electrons, and we estimated the value of the Kondo temperature $T_0 \simeq 0.3$ K. We also measured the molecular field constant $\lambda \simeq -0.7\mathrm{T}/\mu_B$ which corresponds to a saturated exchange field $H_{ex} \simeq 1$ T or to an exchange energy $k_B T_{RKKY} \simeq 1.6$ K of the same order of magnitude as the ordering temperature T_N. By measuring the saturated magnetic moment in the antiferromagnetic phase ($T = 0.05$ K) as a function of the magnetic field, we could observe the crossover from the hybridised state at low fields to the hybridisation free state at high fields, reflecting the smearing out of the Kondo resonance by a large magnetic field.

The Mössbauer spectra below and above T_N show line broadenings which were analysed in detail and interpreted as arising from a distribution of small axial strains (of magnitude $0.2 - 0.4$ K) along the <111> directions. These strains probably originate in inhomogeneities of the Au and Cu compositions. This analysis lead us to conclude that the spontaneous Yb^{3+} magnetic moment in the antiferromagnetic phase cannot lie along the <100> direction and suggests that the moment direction is <110>. It would be of interest to check this prediction by a neutron diffraction study of $YbAuCu_4$ below 1 K.

Appendix 1.

We outline here the method and give the wavefunctions used to obtain the magnetic moment μ and the component of the E.F.G. tensor along the moment direction α_Q^Z for a Kramers doublet at $T = 0$ K in the presence of a small exchange (or Zeeman) interaction $\mathcal{H}_{ex}$ and of a small strain $\mathcal{H}_{dis}$.

In cubic symmetry for $J = \frac{7}{2}$, the C.E.F. eigenfunctions are independent of the x parameter [15]. If a fourfold cubic axis is chosen as z-axis, the eigenfunctions write, in the basis $\left\{|m\rangle = |J = \frac{7}{2}, J_z = m\rangle\right\}$:

$$\begin{cases} |\Gamma_6\rangle &= \frac{\sqrt{7}}{2\sqrt{3}}\left|\frac{1}{2}\right\rangle + \frac{\sqrt{5}}{2\sqrt{3}}\left|-\frac{7}{2}\right\rangle \\ |\Gamma_7\rangle &= \frac{\sqrt{3}}{2}\left|\frac{5}{2}\right\rangle - \frac{1}{2}\left|-\frac{3}{2}\right\rangle \\ |\Gamma_8^1\rangle &= \frac{1}{2}\left|\frac{5}{2}\right\rangle + \frac{\sqrt{3}}{2}\left|-\frac{3}{2}\right\rangle \\ |\Gamma_8^2\rangle &= \frac{\sqrt{5}}{2\sqrt{3}}\left|\frac{1}{2}\right\rangle - \frac{\sqrt{7}}{2\sqrt{3}}\left|-\frac{7}{2}\right\rangle \end{cases} \tag{A1.1}$$

If a threefold cubic axis is chosen as z-axis:

$$\begin{cases} |\Gamma_6\rangle &= \frac{\sqrt{5}}{3\sqrt{6}}\left|-\frac{7}{2}\right\rangle - \frac{\sqrt{7}}{3\sqrt{3}}\left|-\frac{1}{2}\right\rangle - \frac{\sqrt{35}}{3\sqrt{6}}\left|\frac{5}{2}\right\rangle \\ |\Gamma_7\rangle &= -\frac{\sqrt{7}}{3\sqrt{2}}\left|-\frac{7}{2}\right\rangle - \frac{\sqrt{5}}{3}\left|-\frac{1}{2}\right\rangle + \frac{1}{3\sqrt{2}}\left|\frac{5}{2}\right\rangle \\ |\Gamma_8^1\rangle &= \left|-\frac{3}{2}\right\rangle \\ |\Gamma_8^2\rangle &= \frac{\sqrt{14}}{3\sqrt{3}}\left|-\frac{7}{2}\right\rangle - \frac{\sqrt{5}}{3\sqrt{3}}\left|-\frac{1}{2}\right\rangle + \frac{2\sqrt{2}}{3\sqrt{3}}\left|\frac{5}{2}\right\rangle \end{cases} \tag{A1.2}$$

The Kramers conjugate of each state $|\psi\rangle = \sum_m a_m|m\rangle$ is given by: $|\bar{\psi}\rangle = \sum_m (-1)^{\frac{7}{2}-m} a_m^* |-m\rangle$. The perturbation $\mathcal{H}_{ex}$ lifts the Kramers doublet degeneracy; it is diagonalised first inside the doublet basis, and then the first order corrections to the wavefunctions induced by $\mathcal{H}_{ex} + \mathcal{H}_{dis}$ are calculated using standard perturbation theory. The average values of J_z and $3J_z^2 - J(J+1)$ in the ground state yield the corrections to μ and α_Q^Z respectively, and hence the numbers P and $R(\mathbf{u})$ given in the text, and Q, S and $f(\delta)$ given in table I.

Appendix 2.

We derive here the dynamical broadenings of the ^{170}Yb Mössbauer lineshape of a Kramers doublet in cubic symmetry in the limit of quasi-rapid electronic relaxation, i.e. when the relaxation rate $\frac{1}{T_1}$ is much greater than the hyperfine constant A of the doublet: $\frac{1}{T_1} \gg A$.

Without external magnetic field, the cubic hyperfine Hamiltonian writes: $\mathcal{H}_{hf} = A\mathbf{I} \cdot \mathbf{S}$, $\mathbf{S}$ being the fictitious spin ($S = \frac{1}{2}$) of the doublet which fluctuates with a rate $\frac{1}{T_1}$. The relaxational lineshape writes [22], with $\hbar = 1$:

$$I(p) \propto \frac{p - i\frac{A}{2} + \frac{1}{T_1}}{p^2 + p(\frac{1}{T_1} - \frac{iA}{2}) + \frac{3}{2}A^2}, \tag{A.2.1}$$

where $p = \frac{\Gamma}{2} - i\omega$, Γ being the "static" broadening of the Mössbauer line. Expressing $I(p)$ as a function of the small parameter $u = AT_1$ and expanding to first order in u, one finds:

$$I(p) \propto \frac{1}{p + \frac{3}{2}A^2 T_1}, \tag{A.2.2}$$

which represents a Lorentzian shaped line centered in $\omega = 0$ and having a dynamical broadening: $\Delta\Gamma_R = 3A^2T_1$, as stated in equation (29).

In the presence of a large external magnetic field $\mathbf{H}(\mathcal{H}_{hf} \ll g\mu_\beta H)$, the hyperfine Hamiltonian reduces to its diagonal part: $\mathcal{H}_{hf} = AI_zS_z$, and the relaxational lineshape can be obtained using a stochastic method [23]. When the magnetic field is parallel to the γ-ray propagation direction, the lineshape reduces to the $\Delta I_z = \pm 1$ components: $I(p) = f(A) + f(-A)$, where:

$$f(A) \propto \frac{p - i\frac{A}{2}\mathrm{th}\frac{\Delta}{2k_BT} + \frac{1}{T_1}}{p^2 + \frac{A^2}{4} + \frac{p}{T_1} + \frac{iA}{2T_1}\mathrm{th}\frac{\Delta}{2k_BT}}, \tag{A2.3}$$

Δ being the Zeeman splitting of the doublet: $\Delta = g\mu_B H$. Expanding to first order in the small parameter $u = AT_1$, one obtains:

$$f(A) = \frac{1}{p + \frac{iA}{2}\mathrm{th}\frac{\Delta}{2k_BT} + \frac{A^2T_1}{4}(1 - \mathrm{th}^2\frac{\Delta}{2k_BT})} \tag{A2.4}$$

This represents a Lorentzian shaped line at an energy $\omega = -\frac{A}{2}\text{th}\frac{\Delta}{2k_BT}$ with a dynamical broadening:

$$\Delta\Gamma_R = \frac{A^2T_1}{2}(1 - \text{th}^2\frac{\Delta}{2k_BT}) \quad \text{(A2.5)}$$

as stated in equation (30). The term $f(-A)$ yields a line at an energy $\omega = \frac{A}{2}\text{th}\ \frac{\Delta}{2k_BT}$ with the same dynamical broadening.

References

[1] BRANDT N.B., MOSHCHALKOV V.V., *Adv. Phys.* **33** (1984) 373.

[2] STEGLICH F., *J. Phys. Chem. Solids* **50** (1989) 225.

[3] DONIACH S., *Physica B* **91** (1977) 231.

[4] COQBLIN B., SCHRIEFFER R., *Phys. Rev.* **185** (1969) 847.

[5] BONVILLE P., HODGES J.A., HULLIGER F., IMBERT P., OTT H.R., *J. Magn. Magn. Mat.* **62-63** (1987) 621.

[6] BONVILLE P., HODGES J.A., HULLIGER F., IMBERT P., JEHANNO G., MARIMON da CUNHA J.B., OTT H.R., *Hyperfine Interactions* **42** (1988) 381.

[7] ROSSEL C., YANG K.N., MAPLE M.B., FISK Z., ZIRNGIEBL E., THOMPSON J.D., *Phys. Rev. B* **35** (1987) 1914.

[8] According to our definition of the Kondo temperature: $T_0 = J(J+1)g_J^2\mu_B^2/3k_B\chi(0)$ where $\chi(0)$ is the magnetic susceptibility at $T = 0$ K, and $J = 7/2$ and $g_J = 8/7$ for Yb^{3+}, the T_0 of reference [7] is bigger than ours by a factor $4\pi/(2J+1) = 1.57$.

[9] SEVERING A., MURANI A.P., THOMPSON J.D., FISK Z., LOONG C.K., *Phys. Rev. B* **41** (1990) 1739.

[10] SEVERING A., thesis, Köln (1989) (unpublished).

[11] ZWICKNAGL G., ZEVIN V., FULDE P., *Z. Phys. B - Condensed Matter* **79** (1990) 365.

[12] The C constant for $^{170}Yb^{3+}$ has been determined from the precise measurement of the hyperfine constant associated with the Γ_7 state for Yb^{3+} impurities in metallic and insulating hosts (see Bonville P., Imbert P., Jéhanno G., Gonzalez-Jimenez F., Hartmann-Boutron F. *Phys. Rev. B* **30** (1984) 3672). The found value is: $A(\Gamma_7) = (893 \pm 5)$MHz, hence $C = \frac{A(\Gamma_7)}{g(\Gamma_7)g_n\mu_n} = (102 \pm 3)\text{T}/\mu_B$.

[13] ORBACH R.L., STAPLETON H.J., in "Electron spin relaxation in EPR", S. Geschwind Ed. (Plenum Press, 1972.)

[14] HERPIN A., in "Théorie du magnétisme" (P.U.F, 1968).

[15] LEA K.R., LEASK M.J.M., WOLF W.P., *J. Phys. Chem. Solids* **23** (1962) 1381.

[16] BESNUS M.J., MEYER A., private communication.

[17] ADROJA D.T., MALIK S.K., PADALIA B.D., VIJAYARAGHAVAN R., *J. Phys. C* **20** (1987) L307.

[18] BLOCH J.M., DAVIDOV D., *Phys. Rev. B* **26** (1982) 3631.

[19] BONVILLE P., CONTE R., *J. Phys. France* **46** (1985) 1553.

[20] KANG J.S., ALLEN J.W., ROSSEL C., SEAMAN C.L., MAPLE M.B., *Phys. Rev.* B **41** (1990) 4078.

[21] SIEMANN R., COOPER B.R., *Phys. Rev. Lett.* **44** (1980) 1015;
COOPER B.R., *J. Magn. Magn. Mat.* **29** (1982) 230.

[22] CHOPIN C., SPANJAARD D., HARTMANN-BOUTRON F., *J. Phys. Colloq. France* **37** (1976) C6-73.

[23] NOWIK I., *Phys. Lett.* **24A** (1967) 487.